

3-1-2016

Comparing magnetostructural transitions in Ni₅₀Mn_{18.75}Cu_{6.25}Ga₂₅ and Ni_{49.80}Mn_{34.66}In_{15.54} Heusler alloys

Igor Dubenko
Southern Illinois University Carbondale

Alexander Granovsky
Lomonosov Moscow State University

Erkki Lahderanta
LUT University

Maxim Kashirin
Voronezh State Technical University

Vladimir Makagonov
Voronezh State Technical University

See next page for additional authors

Follow this and additional works at: https://repository.lsu.edu/physics_astronomy_pubs

Recommended Citation

Dubenko, I., Granovsky, A., Lahderanta, E., Kashirin, M., Makagonov, V., Aryal, A., Quetz, A., Pandey, S., Rodionov, I., Samanta, T., Stadler, S., Mazumdar, D., & Ali, N. (2016). Comparing magnetostructural transitions in Ni₅₀Mn_{18.75}Cu_{6.25}Ga₂₅ and Ni_{49.80}Mn_{34.66}In_{15.54} Heusler alloys. *Journal of Magnetism and Magnetic Materials*, 401, 1145-1149. <https://doi.org/10.1016/j.jmmm.2015.11.025>

This Article is brought to you for free and open access by the Department of Physics & Astronomy at LSU Scholarly Repository. It has been accepted for inclusion in Faculty Publications by an authorized administrator of LSU Scholarly Repository. For more information, please contact ir@lsu.edu.

Authors

Igor Dubenko, Alexander Granovsky, Erkki Lahderanta, Maxim Kashirin, Vladimir Makagonov, Anil Aryal, Abdiel Quetz, Sudip Pandey, Igor Rodionov, Tapas Samanta, Shane Stadler, Dipanjan Mazumdar, and Naushad Ali

Comparing magnetostructural transitions in $\text{Ni}_{50}\text{Mn}_{18.75}\text{Cu}_{6.25}\text{Ga}_{25}$ and $\text{Ni}_{49.80}\text{Mn}_{34.66}\text{In}_{15.54}$ Heusler alloys

Igor Dubenko¹, Alexander Granovsky², Erkki Lahderanta³, Maxim Kashirin⁴, Vladimir Makagonov⁴, Anil Aryal¹, Abdiel Quetz¹, Sudip Pandey¹, Igor Rodionov², Tapas Samanta⁵, Shane Stadler⁵, Dipanjan Mazumdar¹, and Naushad Ali¹

¹Department of Physics, Southern Illinois University, Carbondale, IL 62901 USA

²Faculty of Physics, Lomonosov Moscow State University, Moscow 119991, Russia

³Lappeenranta University of Technology, 53851, Finland

⁴Voronezh State Technical University, Voronezh 394026, Russia

⁵Department of Physics & Astronomy, Louisiana State University, Baton Rouge, LA 70803 USA

ABSTRACT

The crystal structure, magnetic and transport properties, including resistivity and thermopower, of $\text{Ni}_{50}\text{Mn}_{18.75}\text{Cu}_{6.25}\text{Ga}_{25}$ and $\text{Ni}_{49.80}\text{Mn}_{34.66}\text{In}_{15.54}$ Heusler alloys were studied in the (10-400) K temperature interval. We show that their physical properties are remarkably different, thereby pointing to different origin of their magnetostructural transition (MST). A Seebeck coefficient (S) was found to pass minimum of about $-20\mu\text{V/K}$ in respect of temperature for both compounds. It was shown that MST observed for both compounds results in jump-like changes in S for Ga-based compound and jump in resistivity of about 20 and 200 $\mu\Omega\text{cm}$ for Ga and In –based compounds, respectively. The combined analyzes of the present results with that from literature show that the density of states at the Fermi level does not change strongly at the MST in the case of Ni-Mn-In alloys as compared to that of Ni-Mn-Ga.

INTRODUCTION

The ferromagnetic Heusler alloys with cubic crystal structures of types $L2_1$ or B_2 constitute a class of magnetic materials that is characterized by many physical properties generally related to peculiarities in the electronic structure and magneto-elastic interactions [1, 2]. Remarkable behaviors such as temperature or magnetic field induced first order structural (martensitic) transition (at $T=T_M$), magnetic shape memory effects, exchange bias, giant magnetocaloric effects, magnetoresistance, and giant Hall effects, etc., have been observed in such systems [3-8]. The Heusler alloys have been of great interest for several decades for thermoelectric, magnetic, half-metallic and many other interesting properties [9, 10, 11]. Thus, such alloys are potentially attractive multifunctional materials for applications in microactuators, magnetic sensors, and magnetic refrigeration. In spite of the progress made in recent years in understanding the interplay between the multifunctional properties of Heusler alloys, the detailed mechanisms responsible for their behavior are not well understood. Due to the delicate balance between electronic, ionic, vibration, and magnetic energies, the properties of these alloys are extremely sensitive to changes in intrinsic parameters, such as chemical composition, type of crystal structure, type and volume fraction of the doping elements, as well as on extrinsic parameters, such as fabrication techniques and conditions, annealing temperature, applied magnetic field, pressure, rate of heating and cooling, sequence of measurements, and cycling. On one hand it presents an opportunity to study the desirable properties at ambient temperatures and at accessible magnetic fields. On the other hand, it makes it challenging to discern the factors responsible for specific phenomena.

The Ni_2MnGa and Ni_2MnIn compounds crystalize in cubic austenitic phases. Ni_2MnGa transforms to a tetragonal martensitic phase as a result of a temperature-induced first order

structural (martensitic) transition at about 220 K. The Ni_2MnGa and Ni_2MnIn alloys are collinear ferromagnets below $T_C = 376$ K and 314 K, respectively, [12, 13]. Changes in stoichiometry or chemical composition affect the temperature intervals of the martensitic/austenitic phase stability and magnetic structures of the alloys. In some cases [see in Ref. 3, 5, 14, 15, 16, 17], composition variation results in a magnetostructural phase transition (MST), i.e., in the simultaneous transformation of crystal structure and magnetic state. Several types of MSTs have been observed in Ni-Mn-Ga/In based Heusler alloys [3, 5, 18 and 19]. However, in general Ni-Mn-Ga/In based Heusler alloys can be characterized by two types of MSTs. These are the transitions with cooling between paramagnetic austenitic and ferromagnetic martensitic states, and ferromagnetic austenitic and low magnetization martensitic states. It is widely believed that peculiarities in the electronic structure of the Heusler alloys are responsible for the martensitic transition [1, 2]. This mechanism, which can be associated with a band Jahn-Teller effect [2], must be accompanied with significant changes in the density of states (DOS) at the Fermi level $N(E_F)$. In spite of several calculations confirming this scenario (see for example [20]) there is no experimental evidence for a much larger DOS $N(E_F)$ in the austenitic relative to the martensite phase in Ni-Mn-In –based alloys. In addition, recent data on the electronic specific heat [21], Hall effect [22], and magneto-optical spectra [23] do not show significant differences in the DOS at the Fermi level for austenitic and martensitic phases, at least for the Ni-Mn-In based alloys.

The second possible mechanism for the MST is the appearance of a new vibrational mode originating from a disorder-induced localization of crystal vibrations [24]. This mechanism is well known in non-magnetic Heusler alloys but, as a rule, a new vibration mode arises at quite

low temperatures [24] and, therefore, cannot directly explain MSTs at relatively high temperatures in magnetic Heusler alloys.

Finally, the third possible driving force of the MST is the difference between magnetic energies in the austenitic and martensitic phases. Of course, all three mechanisms are interconnected because it is not possible to change the magnetic state of the material without changing its electronic structure, and the appearance of a new vibrational mode might cause changes in both the electronic structure and magnetic interactions. Nevertheless, the question remains regarding the main driving mechanism of the MST in magnetic Heusler alloys.

It is clear that it is important to study physical properties sensitive to the DOS near the Fermi level (E_F) in order to understand the mechanisms responsible for the MSTs in magnetic Heusler alloys. Among the transport properties, the thermoelectric power (Seebeck coefficient) is the most sensitive to minute details of the DOS in the vicinity of E_F . This is because, in the simplest single-band model, the contribution to the Seebeck coefficient (S) due to elastic scattering is proportional to the derivative of the DOS with respect to energy at the Fermi level [25]. Thus, the changes in the value of S induced by temperature and magnetic field, or as a result of compositional variation, may be considered as directly related to the changes in the DOS near E_F . The thermoelectric power (TEP) of $Ni_{2+x}Mn_{1-x}Ga$ has been studied in Ref. [26-28]. Negative values of the S -coefficient (of about $-(10-20) \mu V/K$), indicating electron-type carriers in thermoelectric transport, have been observed in the temperature interval of (4-400) K. Sharp changes in the TEP with temperature hysteresis were observed near T_M . The Seebeck coefficient was also found to pass a broader minimum in the interval (180- 220) K which was attributed to the existence of a pseudo-gap in the DOS in these alloys. The interpretation of the TEP data for magnetic alloys is not straightforward because of the multiband character of their electronic

structures at the Fermi level, sd-hybridization, spin polarization, and inelastic scattering contributions. The latter was completely ignored in discussions of the TEP in $\text{Ni}_{2+x}\text{Mn}_{1-x}\text{Ga}$ [26-28]. It is also true for the TEP interpretation for Ni-Mn-Sn [29] and Ni-Mn-In alloys [30]. The TEP of $\text{Ni}_{50}\text{Mn}_{34}\text{In}_{16}$ has been studied in Ref. [30]. It has been found that $S(T)$ curve is characterized by the very narrow peak and sharp changes in value just below T_C and T_M , respectively. By contrast to Ni-Mn-Ga alloys no wide minimum was observed below T_M and $S(T)$ was linear at 2.5-150 K without any signature of phonon drag effect.

Here we report the results on the investigation of the crystal structure, magnetic and transport properties, including resistivity and Seebeck coefficient, of alloys with different types of MSTs, specifically, those representative of Ni-Mn-Ga and Ni-Mn-In based Heusler alloys. The aim of this work is to investigate and compare the transport properties of polycrystalline $\text{Ni}_{50}\text{Mn}_{18.75}\text{Cu}_{6.25}\text{Ga}_{25}$ and $\text{Ni}_{49.80}\text{Mn}_{34.66}\text{In}_{15.54}$ alloys that undergo a MST (with heating) from a ferromagnetic martensitic to a paramagnetic austenitic state, and from a low magnetization martensitic state to a ferromagnetic austenitic state, respectively, in order to understand the basic mechanisms of the MST. The chemical compositions of the alloys were chosen to ensure that the MST was close to room temperature.

EXPERIMENTAL TECHNIQUES

Polycrystalline buttons of $\text{Ni}_{50}\text{Mn}_{18.75}\text{Cu}_{6.25}\text{Ga}_{25}$ and $\text{Ni}_{49.80}\text{Mn}_{34.66}\text{In}_{15.54}$ were prepared by arc-melting in a high-purity argon atmosphere using 4N purity Ni, Mn, Cu, In, and Ga. For homogenization, the samples were wrapped in tantalum foil and annealed at 850 °C for 24 hours under vacuum, and then slowly cooled to room temperature. The phase purity and crystal structures were determined using room temperature X-ray diffraction (XRD) measurements (Cu-

K α radiation). The magnetic properties were measured at temperatures ranging from (10-400) K, and at magnetic fields up to 5 T, using a superconducting quantum interference device magnetometer (SQUID by Quantum Design). The temperature dependence of the magnetization, $M(T)$, was carried out during heating after the samples were cooled from 380 K to 10 K at zero magnetic field (ZFC), and during a field-cooling cycle (FCC). The $M(T)$ curves were measured in applied fields of 0.01 and 5 T. The resistivity was measured using the four probe method in the temperature interval of (10-350) K. For the Seebeck coefficient measurements, the samples were cut into rectangular parallelepipeds with a typical size of 1.5x1.5x5.0 mm³. Seebeck voltages were detected using a pair of thin Cu wires attached to the sample with silver paint at the same positions as the junctions of the differential thermocouples. All experiments were performed during warming with a rate slower than 20 K/h. The reproducibility of the Seebeck coefficient measurements were better than 2%, while the absolute accuracy of about 15% that mainly arises from the error in the determination of the sample size.

Results and Discussion

Both Ni₅₀Mn_{18.75}Cu_{6.25}Ga₂₅ and Ni_{49.80}Mn_{34.66}In_{15.54} were found to be in a mixture of cubic and tetragonal phases at room temperature, as evident in Fig. 1. The presence of the mixed state is a signature of the temperature-induced structural (martensitic) first order transition originating from crystal phase temperature hysteresis. The $M(T)$ curves also clearly indicate a temperature induced first order transition by the sharp changes in magnetization at $T=T_A/T_M$ and by the temperature hysteresis of ZFC and FCC $M(T)$ curves (see Fig. 2). Analysis of the $M(T,H)$ curves showed that the magnetic transitions at $T=T_A$ are transitions from ferromagnetic to paramagnetic (for Ni₅₀Mn_{18.75}Cu_{6.25}Ga₂₅), and low-magnetization to high magnetization

(ferromagnetic) states (for $\text{Ni}_{49.80}\text{Mn}_{34.66}\text{In}_{15.54}$). Thus, the compounds under investigation show different types of magnetostructural phase transitions.

The electrical resistivity $\rho(T)$ curves of the samples are shown in Fig. 3. The jump-like variation and temperature hysteresis in $\rho(T)$ is clearly visible near the MST. However, the change in resistivity at the MST is much larger (by about three times) in the case of $\text{Ni}_{49.80}\text{Mn}_{34.66}\text{In}_{15.54}$ compared to that for $\text{Ni}_{50}\text{Mn}_{18.75}\text{Cu}_{6.25}\text{Ga}_{25}$. The residual resistivity ($\rho(T=0) \sim 300 \mu\Omega\text{cm}$) was found to be about six times larger for $\text{Ni}_{49.80}\text{Mn}_{34.66}\text{In}_{15.54}$. In the temperature interval above the MST ($T > 275\text{K}$), a resistivity of $(100\text{-}150) \mu\Omega\text{cm}$ was observed for the In-based alloy, which is smaller than the $(230\text{-}250) \mu\Omega\text{cm}$ observed for $\text{Ni}_{50}\text{Mn}_{18.75}\text{Cu}_{6.25}\text{Ga}_{25}$.

Large differences between the compounds have been observed in the differential thermopower, $S(T)$, shown in Fig. 4. The $S(T)$ of $\text{Ni}_{50}\text{Mn}_{18.75}\text{Cu}_{6.25}\text{Ga}_{25}$ exhibits jump-like changes near the MST and a broad minimum far below T_M , which is in qualitative and rough quantitative agreement with data reported for the ternary alloys $\text{Ni}_{2+x}\text{Mn}_{1-x}\text{Ga}$ [26-28]. In the case of the Ni-Mn-In compound, the minimum in $S(T)$ was observed at the temperature of the MST. The change of the slope of $S(T)$ near T_C was clearly detected for the $\text{Ni}_{49.80}\text{Mn}_{34.66}\text{In}_{15.54}$ alloy (see Fig. 4).

Two features of the $\rho(T)$ behavior need to be illuminated before discussing the TEP data. First, in spite of the high value of the resistivity of the In-based alloys ($> 300 \mu\Omega\text{cm}$), metallic type of $\rho(T)$ behaviors were observed for $T < T_A$. This is contrary to Mooij rule [31], according to which, in highly resistive metals with residual resistivity more than $150 \mu\Omega\text{cm}$, the temperature resistance coefficient should be negative. Apparently, this means that Mooij's rule is not valid for ferromagnetic alloys, as has been noted in Ref. [32], and indirectly indicates a weak localization mechanism for this rule [33]. However, it is unclear why the weak localization mechanism is

active at relatively high temperatures. Secondly, the resistivity of both alloys abruptly decrease in value, and the changes in resistivity is much stronger for the Ni-Mn-In Heusler alloy in the vicinity of the MST (i.e., the martensite-austenite transition).

It is well-known that [25] the resistivity of a metallic system can be written as:

$$\rho \propto \frac{1}{[N(E_F)]^3 \tau(E_F)} \propto \frac{V^2}{[N(E_F)]^2} \quad (1)$$

where $\tau(E_F)$ is the relaxation time, a V is the scattering potential. Thus, possible reasons for the decrease in the resistance at the MST can be either the increase in the DOS at the Fermi level, or the reduction of the scattering intensity. These two mechanisms will be considered below in the discussion of the thermopower.

It is common to use Mott formula to describe the thermopower (S) in Heusler alloys [25]:

$$S_1 = -\frac{\pi^2}{3} \frac{k_B^2 T}{|e|} \left[\frac{\partial}{\partial E} \ln \sigma(E) \right]_{E=E_F} \quad (2)$$

where e is the electron charge, k_B is the Boltzmann constant, $\sigma = 1/\rho$ is the electrical conductivity. In the case of the single-band model, and neglecting the possible dependence of the relaxation time on the energy (see (1)), S_1 can be written as:

$$S_1 \propto T \left[\frac{1}{N(E)} \frac{\partial}{\partial E} N(E) \right]_{E=E_F} \quad (3)$$

In the case of a two-band model where the charge carriers are electrons with spin indexes along and opposite to the magnetization, (\uparrow) and (\downarrow), respectively, S_2 can be written as:

$$S_2 = \frac{\sigma_{\uparrow} S_{1\uparrow} + \sigma_{\downarrow} S_{1\downarrow}}{\sigma_{\uparrow} + \sigma_{\downarrow}} \quad (4)$$

If s-electrons are considered to be unpolarized, the d-band is partially filled and $N_{d\uparrow}(E_F) \neq N_{d\downarrow}(E_F)$ when [34]:

$$S_3 = -\frac{\pi^2 k_B^2 T}{3 |e|} \left[\frac{3}{2E_F} - \left(\frac{\partial N_{d\uparrow}(E)}{\partial E} + \frac{\partial N_{d\downarrow}(E)}{\partial E} \right)_{E=E_F} \right] \quad (5)$$

It should be noted that, in all of these modifications of the Mott expression, the Seebeck coefficient depends linearly on the temperature, and a nonlinearity of $S(T)$ can only be associated with the temperature dependence of the DOS (or electron-phonon and electron-magnon drag effects at low temperatures). Thus, it is rather difficult to explain the presence of the wide minimum in the $S(T)$ curves (see Fig. 4) based on these expressions (2-5). Moreover, the Seebeck coefficient calculated using Mott's model happens to be about several $\mu\text{V/K}$ ($S_1 \approx \frac{k_B^2 T}{eE_F}$), which is in good agreement for the case of non-magnetic metals [25, 33], but not

justified for Heusler alloys (see in Fig. 4). However, in addition to contributions from elastic scattering (2-5) in crystalline and amorphous ferromagnetic alloys, there is also a contribution associated with inelastic scattering, which is larger than the elastic term and leads to a minimum in the temperature dependence of the thermopower at $(0.4-0.6)T_C$ [35, 36]. This contribution had been considered in several works [34, 35] and, following Korenblit [36], it can be written as:

$$S_4 = \frac{k_B}{e} \frac{\tau_{\uparrow} - \tau_{\downarrow}}{t} \quad (6)$$

where t is the inelastic scattering relaxation time, and τ_{\uparrow} and τ_{\downarrow} are the elastic scattering relaxation times for spin-up and spin-down electrons, respectively. The inelastic scattering relaxation times have a tendency to approach infinity as $T \rightarrow 0$ K and, as a result, $S(T \rightarrow 0) \rightarrow 0$. At $T \gg T_C$, the spin polarization disappears and, as a result, $\tau_{\uparrow} - \tau_{\downarrow}$ and $S(T \gg T_C) \rightarrow 0$. Thus, the TEP for S_4 tends to zero with increasing temperature for $T > T_C$ and, therefore, passes through a minimum at an intermediate temperature. In addition, the term resulting from inelastic scattering

is about $S_4 \approx \frac{k_B T}{e T_C}$, i.e., $\frac{E_F}{k_B T_C}$ times larger than from elastic scattering, and therefore may be considered as the main contribution in ferromagnetic alloys [36].

Coming back to the experimental data on the thermopower, both alloys show large TEP values that are difficult to explain in the framework of the Mott formula for elastic scattering. Especially considering that, according to the calculations of the electronic structure of these alloys, no narrow peaks in the DOS have been revealed near the Fermi energy [37, 38]. For Ni-Mn-Ga-based alloys, the minimum of the $S(T)$ curve was observed at a temperature of about $(0.4-0.6)T_A$ (see in Figure 4) and $T_C=T_A$ or T_M . The minimum of $S(T)$ at the temperature of $(0.4-0.6)T_C$ is typical for ferromagnetic alloys and consistent with inelastic scattering mechanisms, see eq. (6) and in [Ref. 35]. Moreover, the resistivity of Ni-Mn-Ga alloys shows no features in the vicinity of the minimum of $S(T)$ (see in Figs. 3 and 4). Thus, there is no experimental evidence that this minimum is due to gradual changes in electronic structure with temperature. The inelastic contribution to the TEP is not the only source. Slight changes in the curvature of the TEP near the Curie temperature, and the spike- and jump-like anomalies observed for Ni-Mn-Ga-based Heusler alloys in the vicinity of the MST (Fig. 4) might be due to the elastic contribution, namely, due to slight changes in the DOS. Indeed, one can see from (1) and (2) that an increase in the DOS at the Fermi level for a triangle peak or half-elliptical shape of the DOS should cause simultaneous decreases in both the resistivity and the TEP, and that is the case. Therefore, these data confirm that the MST in the Ni-Mn-Ga alloys is accompanied by slight changes in the DOS at the Fermi level, which is possible because of the redistribution of s and d states, and is consistent with a band Jahn-Teller model for the MST.

The situation drastically changes in the case of the Ni-Mn-In -based Heusler alloys. The position of the TEP minimum, or jump in the TEP, is almost identical to the temperature of the

MST (T_A or T_M), where the resistance decreases/increases by almost three-fold. Is it possible that this behavior is entirely due to strong changes in the DOS? The specific heat measurements in the Ni-Mn-In alloys show that the difference in the DOS at the Fermi level in the austenite and martensite is only about 10%, which cannot explain the resistivity changes (see (1)). Such small differences are not consistent with the relatively deep minimum of the TEP.

As mentioned earlier, the Hall Effect and magneto-optical data do not show strong changes in the DOS at the MST in these alloys [22, 23]. Therefore, it is reasonable to conclude that the change in resistivity at the MST in the Ni-Mn-In alloys is mostly due to changes in the scattering intensity (see (1)). The large resistivity in martensitic phase can be due to the scattering by the twin boundaries. It might also be possible that the scattering potential in the cubic AP is much smaller than in the MP with lower symmetry. Finally, the magnetic contribution to the resistivity in the Ni-Mn-In alloys can be extremely large in martensitic phase due to antiferromagnetic correlations resulting in low magnetization state below T_A or T_M (see Fig. 2). One can therefore see that there is no definite answer regarding the origin of the sharp decrease of resistivity at the MST, and further investigations are needed.

The TEP behavior is much more complicated in Ni-Mn-In, and is due to several contributions: inelastic scattering, elastic intraband s-s, d-d and s-d scattering. The temperature of the minimum of the $S(T)$ is about $0.7T_C$ of the austenitic phase, as can be expected for the inelastic contribution. The low magnetization state of the martensite is a mixture of austenitic and martensitic phases with strong antiferromagnetic correlations, which changes to a ferromagnetic martensite with decreasing temperature (Fig. 1). Therefore, spin polarization might exist at $T < T_M$ and might change at the MST, which is the main factor responsible for the inelastic contribution (6). The large value of S also indicates the importance of this contribution.

But the non-monotonic TEP behavior near the MST, and the change of slope at T_c , of the austenite show that contributions from elastic scattering (3) or (4) add to the inelastic contribution.

Thus, the combined analyzes of the present results with that from literature show that the DOS at the Fermi level does not change strongly at the MST in the case of Ni-Mn-In alloys as compared to that of Ni-Mn-Ga.

Acknowledgements: This work was supported by the Office of Basic Energy Sciences, Material Science Division of the U.S. Department of Energy, DOE Grant No. DE-FG02-06ER46291 (SIU) and DE-FG02-13ER46946 (LSU) and by the Russian Foundation for Basic Research No. 15-02-01976 (MSU).

References:

- [1] P.Entel, V.D.Buchelnikov, V.V.Khovailo, A.T.Zayak, W.A. Adeagbo, M. E. Gruner, H.C.Herper, E.F.Wassermann, *J. Phys. D: Appl. Phys.* **39** (2006) 865–889.
- [2] P.J. Brown, A.Y. Bargawi, J. Crangle, K.-U. Neumann, K.R.A. Zibeck, *J. Phys. Condens. Matter.* **11** (1999) 4715.
- [3] T.Krenke, M.Accet, E.F.Wassermann, X.Moya, L.Manosa, A.Planes, *Phys. Rev.* **B 73** (2006) 174413.
- [4] I. Dubenko, M.Khan, A.K.Pathak, B.R.Gautam, S.Stadler, N.Ali, *J. Magn. Magn. Mater.* **321** (2009) 754–757.
- [5] I. Dubenko, T.Samanta, A.KumarPathak, A.Kazakov, V.Prudnikov, S.Stadler, A.Granovsky, A.Zhukov, N.Ali, *J. Magn. Mag. Mater.* **324** (2012) 3530–3534.
- [6] I. Dubenko, A.K.Pathak, S.Stadler, N.Ali, Ya.Kovarskii, V.N.Prudnikov, N.S. Perov, A.B.Granovsky, *Phys. Rev. B* **80** (2009) 092408.
- [7] A.K. Pathak, M. Khan, B.R. Gautam, S. Stadler, I. Dubenko, N. Ali, *J. Magn. Mater.* **321** (2009) 963–965.
- [8] A. K. Pathak, M. Khan, I. Dubenko, S. Stadler, N. Ali, *Appl. Phys. Lett.* **90**, 262504 (1-3) 2007.
- [9] Y. Gelbstein, N. Tal, A. Yarmek, Y. Rosenberg and M.P. Dariel, S. Ouardi, B. Balke, C. Felser and M. Köhne, *J. Mat. Research* **26** (2011) 1919-1924.
- [10] K. Kirievsky, Y. Gelbstein, D. Fuks, *J. Solid State Chemistry* **203** 247-254 (2013).
- [11] K. Kirievsky, M. Scilmovich, D. Fuks and Y. Gelbstein, *Phys. Chem. Chem. Phys.* **16** 20023 (2014).
- [12] M. Khan, I. Dubenko, S. Stadler, and N. Ali, *J. Phys. Condens. Matter.* **16**, 5259 (2004).
- [13] Y.V. Kudryavtsev, Y.P. Lee, J.Y. Rhee, *Phys. Rev. B* **69** 195104(1-9) (2004).
- [14] S. Stadler, M. Khan, J. Mitchell, N. Ali, A. Gomes, I. Dubenko, A. Takeuchi, A. Guimaraes, *Appl. Phys. Lett.* **88**, 192511(1-3) 2006.
- [15] I. Dubenko, A. Quetz, S. Pandey, A. Aryal, M. Eubank, I. Rodionov, V. Prudnikov, A. Granovsky, E. Lahderanta, T. Samanta, A. Saleheen, S. Stadler, N. Ali, *J. Magn. Mag. Mater.* **383** (2015) 186–189.

- [16] S. Pandey, A. Quetz, A. Aryal, T. Samanta, I. Dubenko, S. Stadler and N. Ali, *J. Appl. Phys.* **117**, 183905 (2015).
- [17] S. Pandey, A. Quetz, A. Aryal, T. Samanta, I. Dubenko, S. Stadler and N. Ali, *J. Appl. Phys.* **117**, 17A737 (2015).
- [18] A. K. Pathak, I. Dubenko, H. E. Karaca, S. Stadler, N. Ali, *Appl. Phys. Lett.* **97** 062505 (2010).
- [19] A. K. Pathak, I. Dubenko, C. Pueblo, S. Stadler, and N. Ali, *Appl. Phys. Lett.* **96** 172503 (2010).
- [20] S. Fuji, S. Ishida, S. Asano *J. Phys. Soc. Japan* **58**, 3657 (1989).
- [21] T. Kihara, X. Xu, W. Ito et al., *Phys. Rev B* **90**, 214409 (2014).
- [22] A. B. Granovskii, V. N. Prudnikov, A. P. Kazakov, A. Zhukov, and I. Dubenko, *JETP* **115** (5) 805-814 (2012).
- [23] E. Ganshina, A. Novikov, V. Chernenko, J. Barandiaran, E. Cesari, I. Rodionov, I. Titov, V. Prudnikov, A. Granovsky, *Solid State Phenomena*, **233-234**, 225 (2015).
- [24] M. Stipcich, J. Marcos, L. Manosa, A. Plane, R. Romero, *Phys. Rev. B* **68**, 214302 (2003).
- [25] N. F. Mott and E. A. Davis, *Electronic Processes in Non-crystalline Materials* (Clarendon, Oxford, 1971), p.47.
- [26] Y. K. Kuo, K. M. Sivakumar, and H. C. Chen, J. H. Su, and C. S. Lue, *Phys. Rev. B* **72**, 054116 (2005).
- [27] K. R. Priolkar, P. A. Bhoje, S. D. Sapeco, and R. Paudel, *Phys. Rev. B* **70**, 132408 (2004).
- [28] N. I. Kourov, V. V. Marchenkov, V. G. Pushin, K. A. Belozerova, *JETP* **144** (2013) 141-146.
- [29] K. Koyama, T. Igarashi, H. Okada, K. Watanabe, T. Kanomata, R. Kainuma, W. Ito, K. Oikawa, K. Ishida, *J. Magn. Mag. Mater.* **310** (2007) e994–e995.
- [30] L. S. Sharath Chandra, M. K. Chattopadhyay, V. K. Sharma, S. B. Roy, *Phys. Rev. B* **81**, 195105 (2010).
- [31] Mooij J.H., *Electrical*, *Phys. Stat. Sol.* **17**(2) (1973) 521–530.

- [32] V. V. Khovaylo, T. Omori, K. Ando, X. Xu, and R. Kainuma, A. P. Kazakov, V. N. Prudnikov, E. A. Gan'shina, A. I. Novikov, Yu. O. Mikhailovsky, D. E. Mettus, A. B. Granovsky, Phys. Rev. B **87**, 174410 (2013).
- [33] V.F. Gantmakher et al., JETP Lett. **94** , 626 (2011).
- [34] F.J. Blatt, P.A. Shroeder, C.L. Foiles, D. Creig, Thermoelectric power of metals, 1976, p.264.
- [35] W.H. Kettler, S.N. Kaul, M. Rosenberg, Phys. Rev. B **39**, 6140 (1989).
- [36] I.Ya. Korenblit et al., J. Physics F: Metal Phys **12** No.7 1259 (1982).
- [37] C.L. Tan, Y.W. Huang, X.H. Tian et al., APL **100**, 132402 (2012).
- [38] Y. K. Kuo, K. M. Sivakumar, H. C. Chen, J. H. Su, C. S. Lue, Phys. Rev. B **72**, 054116 (2005).

Figure Captions:

Figure 1. Room temperature XRD patterns of $\text{Ni}_{50}\text{Mn}_{18.75}\text{Cu}_{6.25}\text{Ga}_{25}$ and $\text{Ni}_{49.80}\text{Mn}_{34.66}\text{In}_{15.54}$

Figure 2. Temperature dependencies of ZFC and FC magnetization of $\text{Ni}_{50}\text{Mn}_{18.75}\text{Cu}_{6.25}\text{Ga}_{25}$ and $\text{Ni}_{49.80}\text{Mn}_{34.66}\text{In}_{15.54}$ obtained at $H=100$ Oe on heating (open symbols) and cooling (closed symbols). Arrows indicate the temperatures of direct (T_M) and inverse (T_A) martensitic transitions and ferromagnetic ordering of austenitic (T_C) and martensitic (T_{CM}) phases. $T_{CM}=T_A/T_M$ in the case of Ga-based alloy.

Figure.3. Temperature dependencies of resistivity for $\text{Ni}_{50}\text{Mn}_{18.75}\text{Cu}_{6.25}\text{Ga}_{25}$ and $\text{Ni}_{49.80}\text{Mn}_{34.66}\text{In}_{15.54}$ obtained on heating (open symbols) and cooling (closed symbols). Arrows indicate the temperature of direct (T_M) and inverse (T_A) martensitic transitions and ferromagnetic ordering of the austenitic (T_C) and martensitic (T_{CM}) phases. The $T_{CM}=T_A/T_M$ in the case of the Ga-based alloy.

Figure.4. The differential thermopower of Heusler alloys (1) $\text{Ni}_{50}\text{Mn}_{18.75}\text{Cu}_{6.25}\text{Ga}_{25}$ and (2) $\text{Ni}_{49.80}\text{Mn}_{34.66}\text{In}_{15.54}$ obtained on heating (open symbols) and cooling (closed symbols). Arrows indicate the temperature of the direct (T_M) and inverse (T_A) martensitic transitions and the ferromagnetic ordering of the austenitic (T_C) and martensitic (T_{CM}) phases.

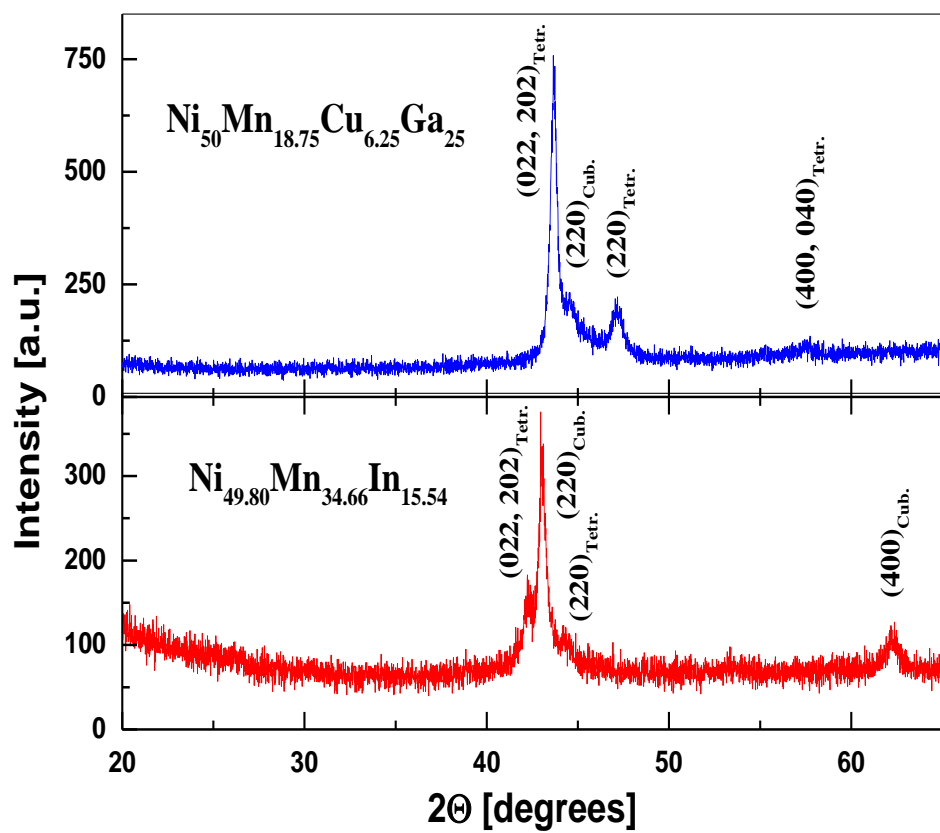


Figure 1. Room temperature XRD patterns of $\text{Ni}_{50}\text{Mn}_{18.75}\text{Cu}_{6.25}\text{Ga}_{25}$ and $\text{Ni}_{49.80}\text{Mn}_{34.66}\text{In}_{15.54}$.

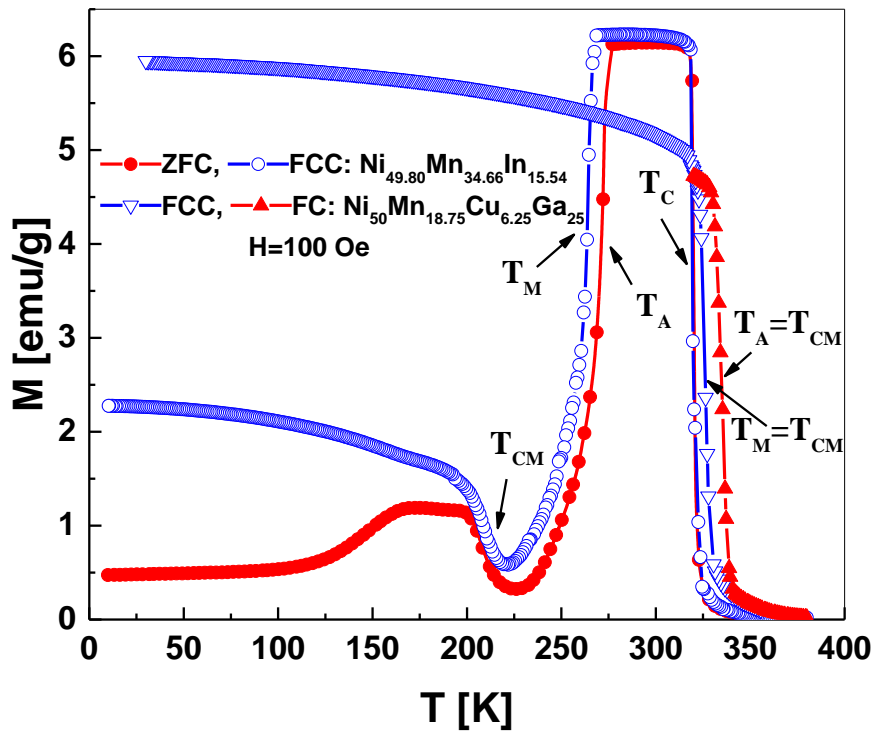


Figure 2. Temperature dependencies of ZFC and FC magnetization of $\text{Ni}_{50}\text{Mn}_{18.75}\text{Cu}_{6.25}\text{Ga}_{25}$ and $\text{Ni}_{49.80}\text{Mn}_{34.66}\text{In}_{15.54}$ obtained at $H=100$ Oe on heating (open symbols) and cooling (closed symbols). Arrows indicate the temperatures of direct (T_M) and inverse (T_A) martensitic transitions and ferromagnetic ordering of austenitic (T_C) and martensitic (T_{CM}) phases. $T_{CM}=T_A/T_M$ in the case of Ga-based alloy.

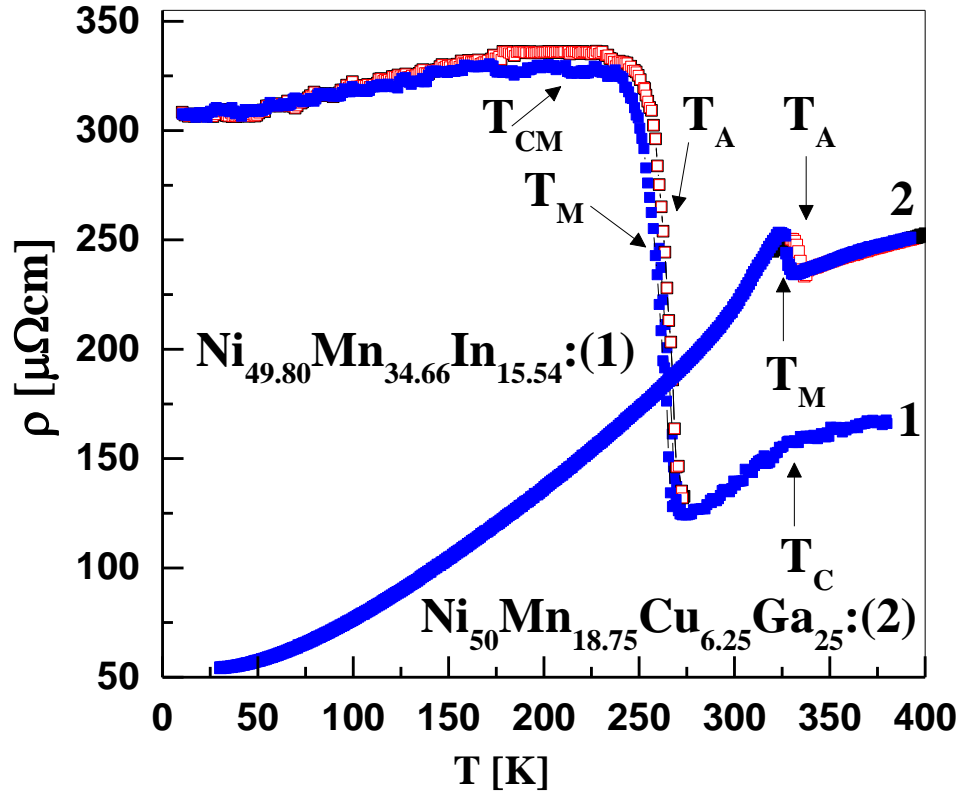


Figure.3. Temperature dependencies of resistivity for $\text{Ni}_{50}\text{Mn}_{18.75}\text{Cu}_{6.25}\text{Ga}_{25}$ and $\text{Ni}_{49.80}\text{Mn}_{34.66}\text{In}_{15.54}$ obtained on heating (open symbols) and cooling (closed symbols). Arrows indicate the temperature of direct (T_{M}) and inverse (T_{A}) martensitic transitions and ferromagnetic ordering of the austenitic (T_{C}) and martensitic (T_{CM}) phases. The $T_{\text{CM}}=T_{\text{A}}/T_{\text{M}}$ in the case of the Ga-based alloy.

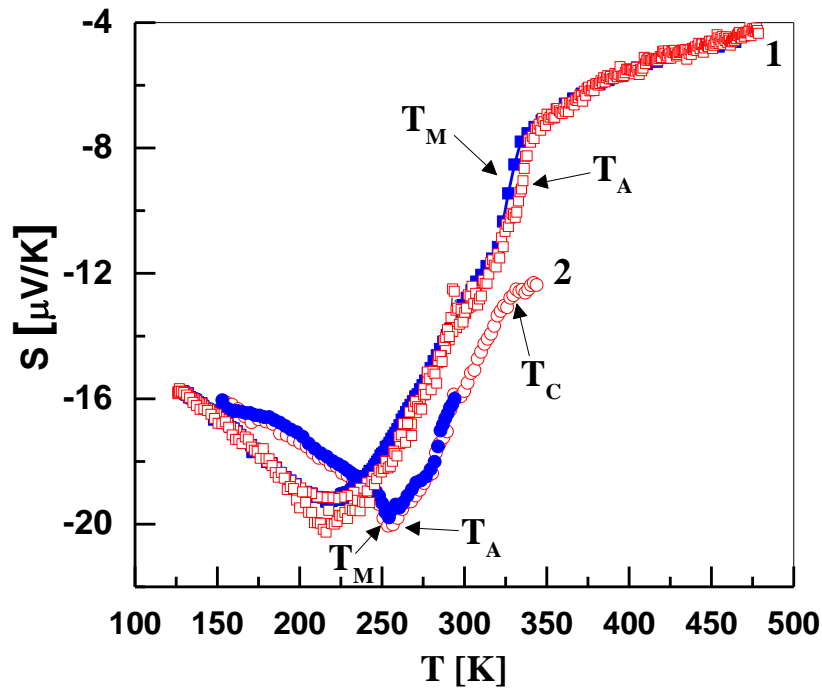


Figure.4. The differential thermopower of Heusler alloys (1) $\text{Ni}_{50}\text{Mn}_{18.75}\text{Cu}_{6.25}\text{Ga}_{25}$ and (2) $\text{Ni}_{49.80}\text{Mn}_{34.66}\text{In}_{15.54}$ obtained on heating (open symbols) and cooling (closed symbols). Arrows indicate the temperature of the direct (T_M) and inverse (T_A) martensitic transitions and the ferromagnetic ordering of the austenitic (T_C) and martensitic (T_{CM}) phases.